Improving biorefinery planning: Integration of spatial data using exact optimization nested in an evolutionary strategy

Tim Schröder[a], Lars-Peter Lauven[a], Jutta Geldermann[a]

[a]: Professur für Produktion und Logistik, Georg-August-Universität Göttingen, Göttingen, Germany

Biorefineries can provide a product portfolio from renewable biomass similar to that of crude oil refineries. To operate biorefineries of any kind, however, the availability of biomass inputs is crucial and must be considered during planning. Here, we develop a planning approach that uses Geographic Information Systems (GIS) to account for spatially scattered biomass when optimizing a biorefinery's location, capacity, and configuration. To deal with the challenges of a non-smooth objective function arising from the geographic data, higher dimensionality, and strict constraints, the planning problem is repeatedly decomposed by nesting an exact nonlinear program (NLP) inside an evolutionary strategy (ES) heuristic, which handles the spatial data from the GIS. We demonstrate the functionality of the algorithm and show how including spatial data improves the planning process by optimizing a synthesis gas biorefinery using this new planning approach.

1.1 Introduction

The transition from traditional fossil-based economies to so-called bioeconomies is attracting increased scientific interest (Golembiewski et al., 2015; Staffas et al., 2013). In a bioeconomy, goods that were once produced from fossil resources are instead produced from biogenous sources (Langeveld and Sanders, 2010). Biorefineries support this transition by providing a product portfolio similar to that of crude oil refineries. To distinguish biorefineries from other, more established biomass conversion plants, the German federal government offers the following definition: “The biorefinery process chain consists essentially of the pre-treatment and preparation of biomass, as well as the separation of biomass components (primary refining) and the subsequent conversion and processing steps (secondary refining)."(Federal Government, 2012). All biorefineries thus consist of a primary refining section, which produces intermediates that are converted to final products in the secondary refining section.

In the German bioeconomy strategy, five different biorefinery concepts with specific inputs are outlined: sugar and starch, lignocellulose, vegetable and algae lipids, synthesis gas, and biogas. Although technology for these five concepts exists, their realization on an industrial scale is hindered by a perceived lack of profitability. The economics of all biorefineries rely heavily on the availability of biomass inputs (Lin et al., 2015; Gold and Seuring, 2011). Thus,

the spatial allocation of available biomass must be considered when planning any biorefinery. Geographic Information Systems (GIS), when used in combination with suitable databases, allow a detailed representation of the spatial availability of biomass. The availability of biomass inputs is important for the decision of where to locate a biorefinery.

However, two further aspects interrelated with the location must also be considered, which renders the problem non-trivial. The optimal plant capacity also depends strongly on the spatial allocation of biomass. Although large capacities reduce specific investments due to economies of scale, they require biomass to be transported further to reach the plant, increasing transportation costs disproportionately. These transportation costs depend once again on the spatial allocation of the inputs. Secondly, the configuration of the biorefinery cannot be decoupled from the capacity. Due to process-specific economies of scale, large refineries have a different optimal configuration than small ones. Therefore, the optimization of the configuration cannot be performed independently from the capacity optimization, which in turn is closely related to the location of the plant and the local biomass availability.

These interdependencies call for an integrated optimization model for location, capacity, and configuration. Thus, the following question entails: How can GIS and detailed spatial data enhance the planning process of a biorefinery's location, capacity, and configuration?

Toward this end, we provide an algorithm to simultaneously optimize the location, capacity, and configuration, using the example of a synthesis gas biorefinery while taking into consideration the spatial distribution of its biomass inputs. Because biorefineries depend primarily on biomass availability and have few additional restrictions, they are not limited to a small number of potential locations. Given that the required permits can be obtained, biorefineries could be built on or near most areas under investigation.

This is especially true within Europe, with its generally well-developed infrastructure and high share of temperate landscapes. This enables us to search for an optimal biorefinery location in a continuous solution space, which legitimately elevates the importance of available biomass relative to other location factors. Nevertheless, larger patches that are unfeasible for biorefinery construction, such as densely populated or protected areas, large bodies of water or mountaintops, may still be excluded from the solution space. In any case, if a biorefinery is built, numerous further bureaucratic steps will have to be taken that will add stricter limitations to the location selection.

Our paper is organized as follows: In Section 1.2, the existing literature concerned with comparable planning problems is laid out. In Section 1.3, the developed optimization algorithm and its components are introduced, before being applied to an exemplary case study in Section 1.4. Results regarding the case study, as well as in terms of algorithm performance, are presented in Section 1.5 and discussed in Section 1.6 before we draw conclusions in Section 1.7.

1.2 Literature review

Optimization models have been used repeatedly to address the planning problems associated with several kinds of biomass conversion plants and supply networks. Such problems are frequently formulated as mixed integer linear programs (MILP). Kim et al. (2011b), for example, used a MILP model to locate and size biomass conversion plants for maximum profit. In a second study, Kim et al. (2011a) added uncertainties to the model using a Monte Carlo simulation. Product portfolio and supply chain optimization for biorefineries was addressed by Mansoornejad et al. (2010), who developed a decision-making framework for designing a product/process portfolio and a supply chain. Bao et al. (2011) focused on biorefinery configuration in a network for optimizing biomass yield or economic potential. Walther et al. (2012) employed a MILP network approach to select the best locations and technologies from ten potential locations and eight different conversion plant technologies and sizes.

Several authors have already used Geographical Information Systems (GIS) to account for spatial aspects in bioenergy-related contexts. Leduc et al. (2010) employed an MILP model to determine cost-optimal locations from a set of discrete locations for ethanol plants having to satisfy a given demand. The configuration of the plants is determined in advance, however, and therefore not subject to optimization. The same basic model was applied to optimize the location and capacity of wood gasification plants in Austria (Leduc et al., 2008). Comber et al. (2015) incorporated the spatial distribution of biomass in optimally locating community-scale anaerobic digesters within a defined area of Great Britain. Furthermore, GIS are routinely used to determine a region's biomass potential and assess (Kurka et al., 2012; Thomas et al., 2013) or optimize the location of plants using these biomasses for energy purposes (Kaundinya et al., 2013; Santibañez-Aguilar et al., 2014; Natarajan et al., 2014; Lin et al., 2013, 2015). Zhang et al. (2011) used a two-staged model that first determines potential facility locations and then minimizes biomass transportation costs to these locations.

Although the aforementioned studies, as well as most mentioned in reviews by Melo et al. (2009) and Owen and Daskin (1998), mainly use linear or mixed-integer models, many of the phenomena that such models have been designed to resemble are actually nonlinear, non-convex, and/or nonsmooth. Such characteristics would actually suggest the use of methods other than MILP. Corsano et al. (2011) include nonlinearities in their MINLP for a bioethanol plant supply chain network and plant configuration. An evolutionary algorithm approach was selected by Rentizelas and Tatsiopoulos (2010) to optimally locate a biorefinery in a continuous, two-dimensional solution space using genetic algorithms and sequential quadratic programming. Wang et al. (2015) combined GIS, mathematical optimization, life-cycle assessment and process engineering software to address the complexity of the biorefinery planning process. Lauven (2014) used nonlinear programming (NLP) to determine the optimal capacity and configuration of a synthesis gas biorefinery under the assumption of evenly distributed average biomass availability - an assumption that does not reflect the regional variability of biomass. Because transport costs for the biomass inputs constitute a large share of biorefinery operating costs, spatial availability does indeed affect a plant's profitability. Naturally, a detailed consideration of spatial biomass availability increases the complexity of the problem. This increased complexity induces the need for heuristics, which are already

being employed in bioenergy contexts. Reche-López et al. (2009) compare different metaheuristics, namely simulated annealing, a genetic algorithm, and particle swarm optimization, to determine the optimal placement of biomass power plants. The discrete problem is solved most efficiently by the algorithm presented in their paper, but a genetic algorithm also performs well. A similar study was published by Vera et al. (2010), who compared genetic algorithms, particle swarm optimization, and honey bee foraging in order to find the optimal location for a biomass power plant. Here, however, the configuration of the plant is not considered, and spatial assumptions are highly simplified, as, e.g., only rectangular biomass supply areas are allowed. Geraili et al. (2014) and Sharma et al. (2013) used metaheuristics, the process engineering software Aspen Plus, and MATLAB to optimize a biorefinery's configuration and capacity for its net present value. However, although Sharma et al. (2013) identify biomass transport as one of the main bottlenecks in biorefineries, they do not explicitly consider the spatial availability of biomass. Ba et al. (2016) offer a comprehensive overview of the decisions modeled and methods used in the performance evaluation of biomass supply chains.

As is clear from our literature review, there has been considerable work done in this field. However, to the best of our knowledge, there is no published model that can plan a biorefinery's location, capacity, and configuration in a continuous solution space while also integrating GIS to consider the spatial availability of biomass at a high resolution. Table 1 provides a selection of publications mentioned in the literature review considering different combinations of biorefinery planning aspects addressed in our approach. The overview illustrates that an approach incorporating all the aspects dealt with in this paper is missing.

Table 1: Selected literature concerned with partial aspects of biorefinery planning

Publication	Location	Capacity	Configuration	GIS	Continuous
Corsano et al. (2011)	■	■		■	(■)
Geraili et al. (2014), Sharma et al. (2013)		■	■		■
Lauven (2014)		■	■		■
Leduc et al. (2008), Leduc et al. (2010)	■	■		■	(■)
Lin et al. (2013), Lin et al. (2015)	■		(■)	■	
Rentizelas and Tatsiopoulos (2010)	■	■		(■)	■
Walther et al. (2012)	■	■	■		
Wang et al. (2015)			■	(■)	

1.3 Development of a biorefinery optimization model based on spatial data

In this section, we first define the problem to be solved: maximizing the Return-on-Investment (ROI) of a biorefinery taking location, capacity, and configuration into account simultaneously.

We then develop a method to solve the problem and go on to describe the materials and tools used to implement the method. The problem to be modeled in the following sections is to locate and scale a biorefinery with the general structure depicted in Figure 1. Biomass is transported from the surroundings to the plant location. At this location, the biomass is converted into marketable products in two refining stages: primary and secondary.

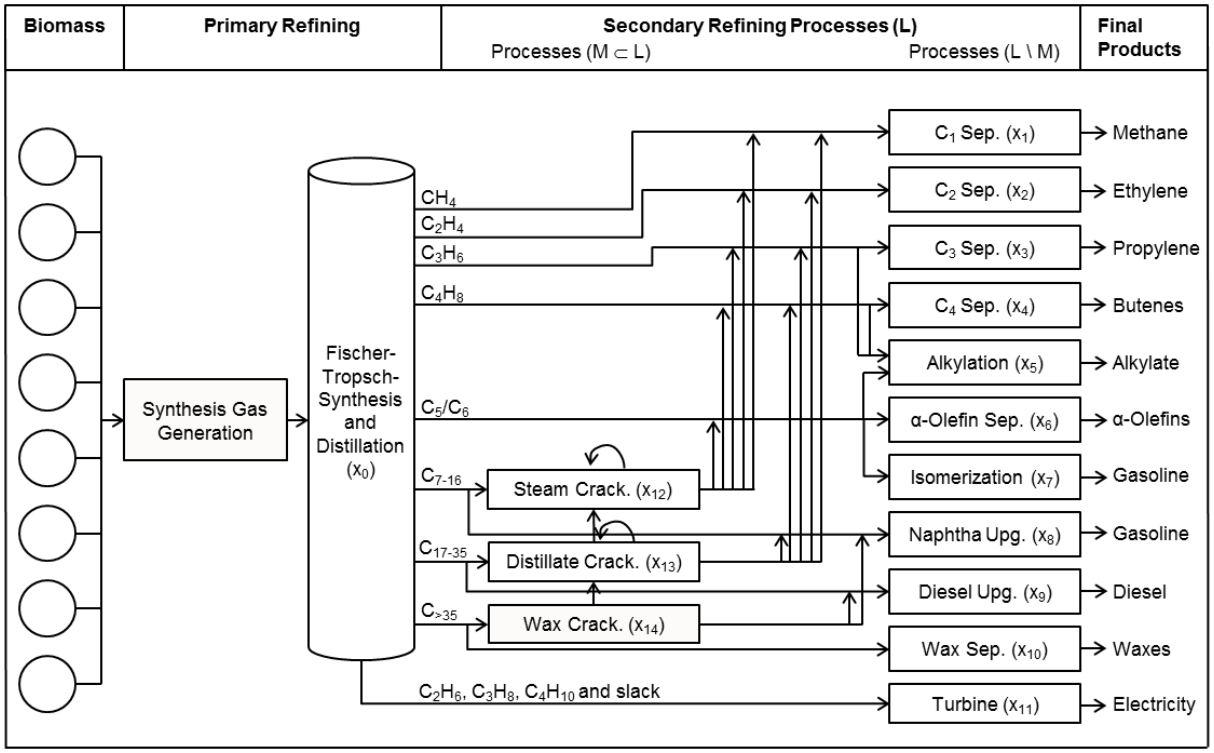

Figure 1: Simplified Structure of the Synthesis Gas Biorefinery with Primary and Secondary Refining

In primary refining, the biomass is gasified and converted to hydrogen and carbon monoxide, together referred to as synthesis gas. The synthesis gas then enters the Fischer-Tropsch-Synthesis, where different hydrocarbons are formed on catalysts. A product stream, containing several raw products, exits primary refining. These raw products can then be separated from the product stream and upgraded into marketable products in secondary refining units. Thus, the capacity of the primary refining defines the overall capacity of the plant. Nevertheless, as the three cracking units do not produce any final products, but instead supply additional input for other secondary refining units, the sum of all secondary refining capacities (x_1 to x_{14} in Figure 1) may be greater than that of the primary refining section (x_0). Because all primary and secondary refining units have individual scaling exponents, different capacities may lead to distinct optimal configurations.

1.3.1 A model that optimizes return-on-investment for a synthesis gas biorefinery in Germany

In this section, we model the problem described above, that is, using GIS to incorporate the spatial availability of biomass into the integrated optimization of Return-on-Investment (ROI) for a synthesis gas biorefinery's location, capacity, and configuration. The ROI is regularly used as an indicator for an investment's profitability in the biorefinery context (Sen et al., 2012;

Schaidle et al., 2011; Mansoornejad et al., 2010). We refrain from the use of more refined, dynamic methods for investment assessments. Indicators such as the net present value (NPV) or the internal rate of return (IRR) are more suitable for planning stages in which detailed assumptions about the investment and future price developments are available. This is not the case in the early planning phase in which the algorithm described here could be applied. Because the algorithm is used for rather conceptual calculations, we believe that the static ROI is sufficient to demonstrate the functionality of the algorithm. Nevertheless, it may be worthwhile to apply dynamic methods when concrete investment projects with profound prognoses on the various costs and market prices are available, as suggested by Chittenden and Derregia (2015).

Sets

G set containing all raw products g

J set containing all biomass supply points j

K set containing all primary refining units k

L set containing all secondary refining units l

M $\subset$ L containing all secondary refining units l not producing any final product i $\in$ I

Parameters

sp_l sales price of final product from secondary refining unit l $\in$ (L \ M) [€ · t^{-1}]

pc_j purchasing cost of biomass at supply point j [€ · t^{-1}]

z_j energy content of biomass at supply point j [MWh]

m_j mass of biomass at supply point j [t]

ξ_j longitude of biomass source j [m]

φ_j latitude of biomass source j [m]

tf fixed transport costs [€ · t^{-1}]

tv variable transport costs [€ · km^{-1} · t^{-1}]

β,γ parameters representing local infrastructure

Ω conversion ratio input energy content to final product mass [MWh · t^{-1}]

Θ factor for the determination of the investment outside battery limits

Ψ cost escalation index

f capital charge rate [% · a^{-1}]

e share of electricity needed for plant operation [%]

α_k base investment of primary upgrading unit k [€]

δ_k scaling exponent of primary upgrading unit k

c_g share of raw product g $\in$ G in the product stream coming from primary refining [%]

α_l base investment of secondary upgrading unit l [€]

δ_l scaling exponent of secondary upgrading unit l

$r_{g,m}$ recycling stream from upgrading unit m $\in$ M supplying raw product g $\in$ G [%]

Variables

ξ_{loc} longitude of the potential location [m]

φ_{loc} latitude of the potential location [m]

x_0 production capacity primary refining [$t \cdot a^{-1}$]

x_l production capacity of secondary refining unit l [$t \cdot a^{-1}$]

h' number of biomass supply sources needed to satisfy the capacity

1.3.1.1 Objective function: maximizing the ROI

In general, the objective function to maximize a biorefinery's ROI is shown in Equation 1. In this section, we will present the objective function and describe the general form of the production system constraints.

$$maxROI = \frac{rev - bc - oc - irc}{inv} \quad (1)$$

where

rev revenues from final product sales

bc biomass purchasing and biomass transportation costs

oc opportunity costs

irc investment related costs

inv total investment for the plant

The first term in the numerator represents the revenues *rev* (Equation 2). The available quantity of the final products equals the capacity of the respective secondary refining unit $x_l \forall\, l \in (L \setminus M)$. The sales prices sp_l for the final products are exogenous and fixed.

$$rev = \sum_{l \epsilon (L \setminus M)} (sp_l \cdot x_l) \quad (2)$$

The second term represents the biomass purchasing and transportation costs *bc*. Before these costs can be calculated, we need to determine how many biomass sources surrounding a potential plant at (ξ_{loc}; φ_{loc}) are required to exactly supply the biomass needed to fuel the capacity x_0 of the plant. To this end, all biomass sources $j \in J$ are sorted in ascending order according to their distances from this potential location. The energy contents z_j of the sources $j \in J$ are accumulated until they suffice to meet the total production capacity x_0. The energy content z_j better reflects the productivity of the input biomass than the mass m_j would. To calculate the production capacity x_0 given in tons of final product in line with z_j, it has to be multiplied with a conversion factor representing the amount of MWh of biomass required to produce one ton of final product. Equation 3 delivers h', the last biomass source required to supply the production capacity of the biorefinery.

$$h' = arg \min_{h \in J} \sum_{j=1}^{h} z_j \mid \sum_{j=1}^{h} z_j \geq \Omega \cdot x_0 \quad (3)$$

Once h' is determined, it can be inserted into Equation 4 as the upper bound of the summation. Equation 4 determines the total biomass costs *bc*, which consist of the biomass purchasing and biomass transport costs. In order to calculate the variable transport costs *tv* for the biomass from any biomass supply point (ξ_j, φ_j) to the potential biorefinery location (ξ_{loc}, φ_{loc}),

the distance on the road has to be approximated. To facilitate the calculation of the Euclidean distances, latitude and longitude are stated in meters.[1] The established weighted *lp* norm based on Minkowski distances described in ReVelle and Eiselt (2005) and Brimberg et al. (2007) does not fit European infrastructures very well (Berens and Körling, 1985). Hence, coefficient β and exponent γ, as parameters representing the regional road infrastructure in the investigated area, are derived through a potential function regression, which delivers the highest coefficient of determination through a point cloud depicting the ratio between the distance on the road, as given by Google Maps and the Euclidean distance between two random points in the considered country or region. The fixed transport costs can be understood as handling costs when loading and unloading the biomass. They only depend on the mass m_j of the biomass at source $j \in J$.

The biomass purchasing costs *bc* are determined by multiplying the mass m_j with the specific purchasing costs pc_j of the biomass available at supply point $j \in J$.

$$bc = \sum_{j=1}^{h\prime} \left(m_j \left(tv \cdot \beta \cdot \sqrt{\left(\xi_{loc} - \xi_j\right)^2 + \left(\varphi_{loc} - \varphi_j\right)^2} \right) + tf + pc_j \right) \tag{4}$$

The third term of the objective function represents the opportunity costs *oc* for the fixed share e of electricity that is not sold, but instead used to operate the plant (Equation 5).

$$oc = x_0 \cdot e \cdot sp_{11} \tag{5}$$

The last term in the numerator in Equation 1 contains the investment-related costs *irc* for both the mandatory primary upgrading units *K* and the optional secondary upgrading units *L*. The potentially large number of configuration variables, which can be part of the optimal solution in a large range of potential capacities, makes a linearization of the problem cumbersome. Therefore, we do not attempt to linearize these economies of scale functions but attempt so solve the problem in its nonlinear form (Equation 6). The gross investment, the two sums at the end of Equation 6, is multiplied with a factor for the determination of additional investment outside battery limits (Θ) and a cost escalation index over time (Ψ) to receive the net investment. The net investment is then multiplied with the capital charge rate f to determine the annual investment related costs.

The parameters for scale effects used in this work are adapted representations of the usual ratio of new over old capacity. The ratio expression is simplified by determining a base investment value for a capacity of one ton per year in a first step (Towler and Sinnott, 2013). This is done to subsequently omit the old capacity in the denominator, which then becomes 1 as well.

$$irc = f \cdot \Theta \cdot \Psi \cdot \left(\sum_{k \in K} \left(a_k \cdot {x_0}^{\delta_k} \right) + \sum_{l \in L} \left(a_l \cdot {x_l}^{\delta_l} \right) \right) \tag{6}$$

[1] In simple terms, the coordinates are given in meters from the Greenwich meridian (ξ) and the equator (φ). However, due to the curvature of the earth, the raster has to be adapted to the investigated area, which distorts the distances to the Greenwich meridian and the equator, but keeps the distortions in the investigated area small. A suitable projection must be chosen in the GIS.

Because ROI calculations, as described by Peters et al. (2003), require the division of the expected annual profit value by the investment *inv*, the denominator of Equation 1 is calculated analogously to the investment-related cost.

1.3.1.2 Geography and capacity constraints

A first set of simple constraints is concerned with the location and the capacity of the potential biorefinery. The coordinate tuple (ξ_{loc}, φ_{loc}) of the potential plant must be within the borders of the country (or region) the plant shall be located in. This constraint can be tested using GIS.

$$(\xi_{\mathrm{loc}}, \varphi_{\mathrm{loc}}) \in feasible\ area \tag{7}$$

Furthermore, the production capacity x_0 of the biorefinery cannot be negative. Nor can it exceed a value that consumes the total residual biomass available in the area under investigation (see Inequality 8).

$$0 \leq x_0 \leq \sum_J \frac{z_j}{\Omega} \tag{8}$$

1.3.1.3 Configuration constraints

Ensuring that the constraints for the plant configuration are not violated is more complex than in the case of the geography and capacity constraints. The configuration constraints ensure adherence to mass balances during the refining stages of the production process.

Methane (CH_4) is part of the product stream from primary refining with a share of c_1 and can be separated from this product stream in the secondary refining unit up to the capacity x_1 (Inequality 9). Additional potential input for this unit comes from the $m \in M$ cracking processes. The return flow $r_{1,m}$ from these cracking units to unit $l = 1$ is expressed as a share of the total size of these cracking units being available for x_1. Thus, the production capacity of marketable methane x_1 must be less or equal to the share of the raw product (c_1) multiplied with the total production capacity x_0 plus the sum of the shares $r_{1,m}$ from the cracking units $m \in M$ multiplied with the corresponding capacities $x_m \forall\ m \in M$.

$$x_1 \leq c_1 \cdot x_0 + \sum_{m \in M} (r_{1,m} \cdot x_m) \tag{9}$$

Analogously, the production capacity x_2 of ethylene (C_2H_4) must be less or equal to its share c_2 multiplied by the total capacity x_0 plus the sum of recycling streams $r_{2,m}$ multiplied with the respective capacities $x_m \forall\ m \in M$ (Inequality 10).

$$x_2 \leq c_2 \cdot x_0 + \sum_{m \in M} (r_{2,m} \cdot x_m) \tag{10}$$

Inequalities 11 and 12 deal with the usage of propylene (C_3H_6) and butenes (C_4H_8). There are two usage options for both these raw products to be transformed into marketable products. They can be purified in the units with the capacities x_3 and x_4. Alternatively, they can be used in the alkylation unit (capacity x_5), where they would make up a certain share (40 percent of the final product mass) of alkylation input to produce high octane additives for petrol.

$$x_3 + 0.4 \cdot \frac{c_4}{c_3 + c_4} \cdot x_5 \leq c_3 \cdot x_0 + \sum_{m \in M} (r_{3,m} \cdot x_m) \quad (11)$$

$$x_4 + 0.4 \cdot \frac{c_4}{c_3 + c_4} \cdot x_5 \leq c_4 \cdot x_0 + \sum_{m \in M} (r_{4,m} \cdot x_m) \quad (12)$$

The hydrocarbons with five to six carbon atoms (C_5/C_6) from primary refining or/and steam cracking have three usage options, represented by the capacities of alkylation (capacity x_5, in which C_5/C_6 hydrocarbons are assumed to make up the remaining 60 percent of inputs), α-olefin production (x_6, base chemicals for polymerization reactions), and isomerization (x_7, producing petrol) (Inequality 13).

$$x_6 + x_7 + 0.6 \cdot x_5 \leq c_5 \cdot x_0 + \sum_{m \in M} (r_{5,m} \cdot x_m) \quad (13)$$

The hydrocarbons in the gasoline range (with 7-16 carbon atoms, Inequality 14) can either be supplied to the naphtha upgrading unit with capacity x_8, which produces petrol, or to the steam cracking unit with capacity x_{12}, where long hydrocarbon chains are cracked into shorter ones. Cracking processes therefore produce additional input for the refining options for shorter hydrocarbon chains, i.e. upgrading processes in Inequalities 9 to 13.

$$x_8 + x_{12} \leq c_6 \cdot x_0 + \sum_{m \in M} (r_{6,m} \cdot x_m) \quad (14)$$

Inequality 15 follows the same principle as Inequality 14 for hydrocarbons suitable for diesel fuel, which range from 17-35 carbon atoms. Diesel-range hydrocarbons, with a share of c_7 of the raw product stream, can either be upgraded to diesel (capacity x_9) or serve as additional input for the other secondary refining units after undergoing distillate cracking (capacity x_{13}).

$$x_9 + x_{13} \leq c_7 \cdot x_0 + \sum_{m \in M} (r_{7,m} \cdot x_m) \quad (15)$$

In analogy to the previous groups of substances, all hydrocarbons with 36 or more carbon atoms, with a share of c_8 of the raw product stream, can either be purified into marketable waxes with a capacity of x_{10} or undergo a specific cracking process with capacity x_{14} (Inequality 16).

$$x_{10} + x_{14} \leq c_8 \cdot x_0 + \sum_{m \in M} (r_{8,m} \cdot x_m) \quad (16)$$

The turbine (capacity x_{11}) acts as a balancing process for the overall system (Equation 17). Because the constraints (9) to (16) are inequalities, it is possible that less than the total amount of raw materials from primary refining is used in the secondary refining units $l \in (L \setminus (M \cup \{11\}))$ to produce final products. Thus, x_{11} acts as a reservoir, collecting the slack from the other upgrading units and ensuring the validity of the mass balances. As a result, all the input entering secondary refining is converted to some kind of final product.

$$x_0 = \sum_{l \in (L \setminus M)} (x_l) \quad (17)$$

The second turbine constraint (Inequality 18) ensures that it is large enough to supply the energy needed for the biorefinery production processes. Thus, e defines the minimal share of

the total products produced, that must to be converted into electricity in the turbine to keep the biorefinery independent of external electricity supply.

$$x_{11} \geq e \cdot x_0 \tag{18}$$

Inequalities 19 to 20 pose further restrictions to the alkylation unit with capacity x_5. An alkylation unit's capacity is limited by the available quantities of the two inputs, 40% C_3 and C_4 hydrocarbons on the one hand and 60% C_6 hydrocarbons on the other hand. Furthermore, as the latter statement implies, not the complete *C_5/C_6* product stream is applicable in this process, but only C_6 hydrocarbons which can be aromatized. The share of these specific molecules is assumed to be 25% of the total *C_5/C_6* stream.

$$x_5 \leq \frac{x_0 \cdot c_3 + \sum_{m \in M}\left(x_m \cdot r_{3,m}\right) + x_0 \cdot c_4 + \sum_{m \in M}\left(x_m \cdot r_{4,m}\right)}{0.4} \tag{19}$$

$$x_5 \leq 0.25 \cdot \frac{x_0 \cdot c_5 + \sum_{m \in M}\left(x_m \cdot r_{5,m}\right)}{0.6} \tag{20}$$

Inequality 21 accounts for the fact that only olefins with a double bond in the α position, α-olefins, are available for α-olefin separation. A share of 60% of the total *C_5/C_6* product stream is assumed to be α-olefins, which limits the capacity x_6 of the α-olefin separation unit to 60% of the total amount of *C_5/C_6* available. However, due to uncertainty whether there is a worthwhile quantity of α-olefins in the output streams of the cracking processes, recycling streams from cracking processes $m \in M$ are not considered as applicable for the α-olefin separation.

$$x_6 \leq 0.6 \cdot c_5 \cdot x_0 \tag{21}$$

1.3.2 Evolutionary strategies for solving non-smooth optimization problems

The objective functions for many real-life problems exhibit difficult characteristics, such as a large number of solutions in the solution space, a noisy objective function landscape, and strict constraints to the solution space (Michalewicz and Fogel, 2000). The biorefinery optimization problem at hand exhibits all these characteristics at the same time. The objective function is noisy due to the locally varying biomass availability. Such non-smooth, noisy, or “rough" (Rechenberg, 1994) objective functions are usually solved using heuristics rather than exact optimization algorithms. A first group of heuristics, evolutionary algorithms (EA), was introduced in the 1960s for large optimization problems (Horng et al., 2012). EA are well suited to solve large and difficult problems in a continuous solution space (Mahdavi et al., 2015). All EA are based on the mechanisms of natural selection, as described by Charles Darwin in 1859. Evolutionary strategies (ES), a subgroup of EA, were introduced by Rechenberg (1973). ES work directly with real or integer variables instead of using their binary representations, which makes them suitable for optimization problems with real or large integer numbers. As other GAs, ES operate with a population of λ individuals, feasible solutions, from which the μ fittest solutions, with the highest objective function values are selected to reproduce λ new children in the next generation.

Vesterstrom and Thomsen (2004) show that Darwinian “real-valued Genetic Algorithms" perform better than other meta-heuristics on noisy objective functions. The algorithm described in their article works with two mechanisms: exogenously-given annealing allows fine tuning in the local search in later stages of the algorithm through decreasing of the mutation step length, while arithmetic crossover generates offspring through weighted arithmetic averages of the parents' variable values (Thomsen, 2003). Both mechanisms, the adaption of the mutation step length and the arithmetic crossover correspond to ES. Since both these mechanisms correspond to ES, the “real-valued Genetic Algorithm" can be classified as an ES with external step-length adaption. Thus, ES seem to be well suited for the optimization of noisy objective functions, as given in Equation 1 in Section 1.3.1.

Julstrom (1999) shows that simple Darwinian EA are more effective than most hybrid EA considered in their paper. Only a Lamarckian[2] approach can perform slightly better than the basic Darwinian approach. This Lamarckian approach uses the exact optimization of a subproblem in order to simplify the overall problem, which leads to the best results.

However, when all variables are handled in the ES, the algorithm does not converge towards good solutions, but often settles for corner solutions, even if better starting solutions are provided. This happens because an important prerequisite for ES is missing: the existence of a superior order within the non-smooth objective function landscape. ES can hardly optimize functions that lack an overall, global structure (Muñoz et al., 2015). Even if such a superior order exists in all of the dimensions separately, this requirement can cause trouble when the dimensionality of a problem increases. The overall structure is lost in the interferences of the larger number of dimensions of the objective function (Chu et al., 2011; Omidvar et al., 2015). Moreover, the configuration constraints (mass balances) in our case study on biorefineries are strict, which further complicates the problem (Michalewicz and Fogel, 2000). Consequently, ES alone cannot reliably solve the problem at hand.

1.3.3 Combining ES and NLP for the integrated optimization of a biorefinery

Usually, complex problems that cannot be solved efficiently are decomposed in order to make them solvable. Unfortunately, the location, capacity, and configuration variables of a biorefinery are interdependent. Thus, the problem cannot be fully decomposed into smaller sub-problems over the complete run of the ES (Sayed et al., 2015). However, it is indeed possible to repeatedly decompose and recompose the problem in each iteration and for each of the λ individuals.

By investigating the individual terms of our objective function in the biorefinery decision problem, the initial reason for the application of a heuristic - the non-smoothness of the

[2] In the early 19th century, the French biologist Jean-Baptiste de Lamarck developed an evolutionary concept in which the offspring could inherit experiences made by the parental generation instead of only the genes, as later correctly postulated by Charles Darwin. This concept is transferred to the genetic algorithm by interposing a local search capable of altering the decision variables before the next genetic iteration starts (Julstrom, 1999).

objective function - can be limited to the term given in Equation 4, the calculation of biomass-related costs. The variables in this term, ξ_{loc}, φ_{loc} and x_0, are closely related to the spatially distributed biomass supply points. A small alteration in location or capacity can lead to different, additional, or fewer biomass supply points being used, which in turn leads to noise in the objective function. The remainder of the objective function, however, is smooth. Within the solution space, this part of the objective function, which contains most variables, is continuous and differentiable and thus suited for exact optimization.

This procedure enables us to reduce the number of decision variables handled in the ES to the three variables causing noise: ξ_{loc}, φ_{loc} and x_0. These variables can be handled in the ES very well and show sufficient superior structure.

The remaining variables x_1-x_{14} relating to the configuration of the biorefinery can be determined using exact nonlinear optimization. Hence, the overall optimization is repeatedly decomposed: a top-level ES and a nonlinear program nested inside the ES. The ES handles and fixes variable values for ξ_{loc}, φ_{loc} and x_0 for a single individual solution; the corresponding costs for purchasing and transporting the required quantity of biomass to the potential location are calculated using Equation 4. These costs and the capacity of the whole plant are subsequently passed on to an exact mathematical program, where they are treated as parameters framing the optimization of the biorefinery's configuration. This overall procedure of the algorithm is depicted in Figure 2, where the exact NLP block is inserted into a standard ES procedure.

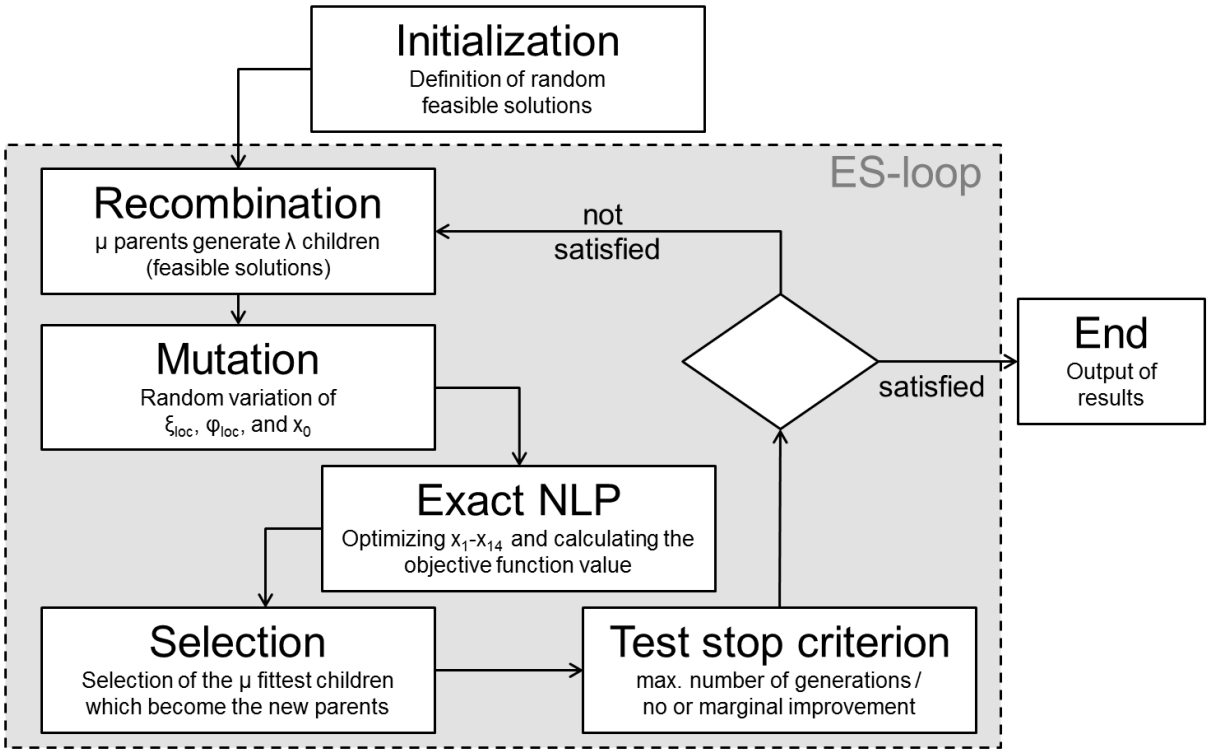

Figure 2: ES Procedure with embedded NLP for integrated optimization of a synthesis gas biorefinery

The more complex constraints representing the mass balances in the biorefinery case study can now be handled completely by the exact optimization algorithm, which is more suitable for dealing with such tight restrictions than the ES. The task of this nonlinear model is now to find the optimal configuration for a preliminarily located and scaled plant at (ξ'_{loc}, φ'_{loc}) with a total

capacity of x'_0. Note that the objective function of this sub-problem is similar to the overall objective function (Equation 1). Temporarily fixing (ξ'_{loc}, φ'_{loc}) and x'_0 in the objective function and all constraints also results in fixed biomass-related costs bc'.

$$maxROI = \frac{\sum_{l\epsilon(L\setminus M)}(sp_l \cdot x_l) - bc' - x'_0 \cdot e \cdot sp_{11} - f \cdot \Theta \cdot \Psi \cdot \left(\sum_{k\in K}\left(I_k \cdot {x'_0}^{\delta_k}\right) + \sum_{l\in L}\left(a_l \cdot {x_l}^{\delta_l}\right)\right)}{\Theta \cdot \Psi \cdot \left(\sum_{k\in K}\left(a_k \cdot {x'_0}^{\delta_k}\right) + \sum_{l\in L}(a_l \cdot {x_l}^{\delta_l})\right)} \quad (22)$$

The resulting NLP can then be solved. The ES retrieves the resulting optimal values unit x_l $\forall l \in L$ and the respective objective function value. This process is performed for all λ individuals. The λ solutions are sorted according to their objective function values. The μ individuals with the highest fitness become the new parental generation. The selected individuals are stored for subsequent analysis. The ES loop starts anew until the maximum number of generations is reached or until there is no substantial improvement in the objective function value. Test runs show that calculating 100 generations suffices for algorithm convergence and supplies a homogeneous group of individuals.

1.3.4 Implementation of the optimization approach

We use several tools to implement the algorithm described above. The superior ES is implemented in Python script and run via PowerShell. Since the ES governs the overall procedure, it must also invoke the other tools used in the process. Both the General Algebraic Modeling System (GAMS), which is used for modeling the NLP, and ArcGIS, which is used for the geographic operation, have Python application programming interfaces (APIs) for such purposes.

GAMS is a mathematical modeling environment provided by the GAMS Development Corporation. It enables clear model formulation and utilization of several different solvers. The Branch and Reduce Optimization Navigator (BARON) is used to solve the NLP described above (Tawarmalani and Sahinidis, 2005; Sahinidis, 2014).

For the geographic operations, we use the popular and commercially available geographic information system ArcGIS, by ESRI Inc. This software contains a large number of geographic tools for processing spatial data. All the tools usually accessed via the graphical user interface can also be accessed directly via the Python API. This allows spatial operations to be performed within the ES. Moreover, ArcGIS is also needed to prepare the geographic input data required for the spatial representation of the biomass input, as described in Section 5.4.1.

1.3.5 Altering location and capacity variables in the ES

Both after initializing the algorithm and after selecting the best solutions found in each iteration, the location and capacity variables are altered in the recombination and mutation step of the ES. The recombination, or crossover, procedure is performed by calculating the weighted averages of two randomly chosen parental variable values. This intermediary recombination method incorporates a factor that randomly assigns weights between -0.25 and 1.25 that add up to 1 for both the parental variables $x^{parent1}$ and $x^{parent2}$. The possible assignment of values

outside the zero-to-one range ensures that the children's parameters do not inevitably converge, and that the average distance of the parental values remains stable (Pohlheim, 1999). The mutation incorporates one strategy variable for each decision variable. These strategy variables influence the expected step length of the mutation, i.e., the expected difference between the decision variable value before and after the mutation. In the course of the algorithm, this strategy variable adapts to allow for good coverage of the solution space in the early stages of the algorithm and a precise approach to the local optimum in the later stages. Thus, these strategy variables act as scaling factors for a standard normal random number, which is then added to the decision variable. After both the recombination and the mutation, the location tuple and capacity are tested for feasibility. In the case of infeasibility, the corresponding step is repeated 25 times. If no feasible solution can be found in 25 attempts, the location/capacity of the first parent is used as the child's variable value. Furthermore, so called comma-selection is applied, which means that each individual can only survive one generation (Rechenberg, 1994).

1.4 Numerical application of the algorithm to an exemplary case study in Germany

To test the influence of spatial data on biorefinery planning, we use the algorithm to locate, scale, and configure a synthesis gas biorefinery in Germany. While eventual convergence toward the global optimum can be guaranteed and proven for some adaptive random search algorithms, this guarantee does not exist for ES (Regis, 2010). By analyzing both the final optimization results and the investigated solutions during the optimization process, we aim to assess whether the algorithm converges reliably towards good solutions. To do this, the values in the sets for products (G), biomass supply points (J), primary (K) and secondary (L) refining units must first be specified. Table 2 shows the raw products $g \in G$ from the primary refining units and their corresponding mass shares c_g in the product stream, which is preliminarily separated into several streams in a distillation unit (Dry, 2004).

Table 2: Raw primary refining product set G with corresponding shares c_g (Dry, 2004)

Index	Raw Product $g \in G$	Share c_g
1	CH_4	8.4%
2	C_2H_4	4.2%
3	C_3H_6	11.6%
4	C_4H_8	9.5%
5	C_5/C_6	16.8%
6	C_7-C_{16}	21.1%
7	C_{17}-C_{35}	16.7%
8	$C_{>35}$	5.3%
9	C_2H_6	3.2%
10	C_3H_8	2.1%
11	C_4H_{10}	1.1%

Table 3 shows the secondary refining units $l \in L$ with their respective base investments a_l and scaling exponents δ_l (Kreutz et al., 2008; Peters et al., 2003; Tijmensen et al., 2002; Towler

and Sinnott, 2013). Furthermore, the two columns on the right show which final products are produced by each of the secondary upgrading units $l \in L$, as well as their corresponding sales prices sp_l in Euros per ton.

Table 3: Properties of upgrading processes and final products with prices

Ind. l	Secondary Refining Unit $l \in L$	Base Invest a_l	Scaling Exp δ_l	Product	Prices sp_l
1	Methane Upgrading	227	0.7	Methane	350
2	C_2-Separation	48,098	0.6	Ethylene	1,604
3	C_3-Separation	45,816	0.6	Propylene	1,574
4	C_4-Separation	16,931	0.6	Butene	1,168
5	Alkylation	39,727	0.67	High Oct. Add.	1,310
6	α-Olefin separation	194,007	0.6	α-Olefins	1,321
7	Isomerization	2,975	0.62	Gasoline	1,182
8	Naphtha Upgrading	12,862	0.625		
9	Distillate Upgrading	5,293	0.55	Diesel	1,161
10	Wax Upgrading	21,124	0.6	Wax	1,896
11	Turbine	2,516	0.75	Electricity	185
12	Naphtha Cracking	1,784	0.55	No final products produced by these processes (M ⊂ L)	
13	Distillate Cracking	1,784	0.55		
14	Wax Cracking	16,821	0.55		

Kreutz et al., 2008; Peters et al., 2003; Tijmensen et al., 2002; Towler and Sinnott, 2013

Table 4 shows the recycling streams from the secondary upgrading units $m \in M$, which provide additional raw products $g \in G$ for subsequent use in the secondary upgrading units $l \in L$. The remaining parts of the recycling streams are used in the turbine (x_{11}).

Table 4: Secondary refining units $m \in M$ producing additional raw products $g \in G$

	$r_{1,m}$	$r_{2,m}$	$r_{3,m}$	$r_{4,m}$	$r_{5,m}$	$r_{6,m}$	$r_{7,m}$	$r_{8,m}$	$\sum_{g=9}^{11} r_{g,m}$
$r_{g,1}$	0.149	0.357	0.179	0.042	0.062	0.144	0	0	0.067
$r_{g,2}$	0.080	0.190	0.140	0.110	0	0.200	0.270	0	0.010
$r_{g,3}$	0	0	0	0	0	0.300	0.650	0	0.050

1.4.1 Preparing the input data

The data processed in ArcGIS, which reflects the spatial allocation of the biomass, comes from the Corine Land Cover (CLC) 2006 (Umweltbundesamt, 2009) dataset. This dataset categorizes the surface of 38 European countries into 44 land cover classes. The most accurate representation is attained by the vector dataset, which contains shapefiles with seamlessly interlocking polygons for all 44 land-cover categories. CLC 2006 depicts the land covers as they were in 2006, which should be sufficiently accurate to demonstrate the approach.

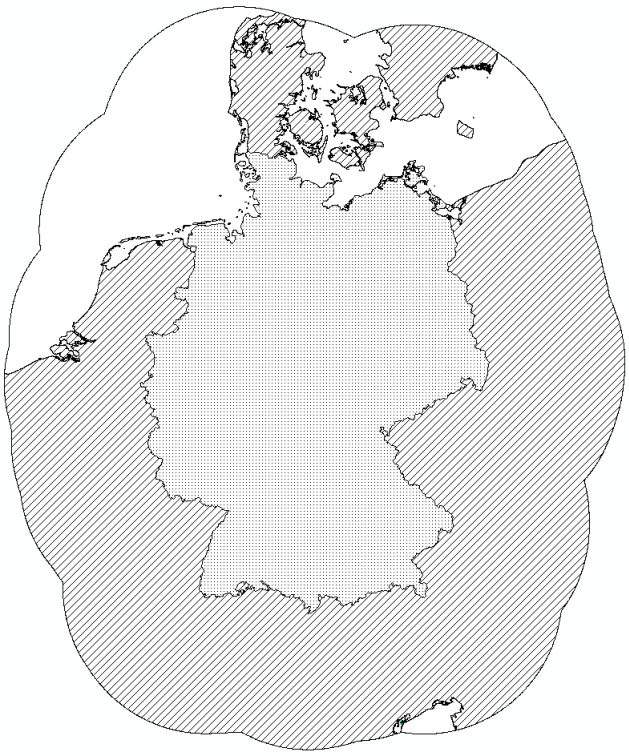

Figure 3: Potential biomass supply area for a biorefinery in Germany

To apply the algorithm and calculate objective function values, the raw CLC 2006 data must undergo several editing steps in the GIS. The aim here is to develop a set J that contains all biomass sources within and around the German borders (see Figure 3) as vectors including their location, type, and quantity. Generally, there are two contradicting goals to pursue when editing the input data. On the one hand, the data should be aggregated to reduce the volume of data to be handled in the algorithm and shorten run time. On the other hand, the spatial distribution of the biomass must be accurate enough to justify the additional calculation efforts compared to highly aggregated discrete models. As described in the following eleven steps, this is achieved by first aggregating the data, where possible, and subsequently maintaining accuracy through selective separation of regions that are too highly aggregated.

1. The potential area supplying biomass is identified and extracted from the database. Especially when working with extensive databases, such as the CLC 2006 database, this step is important to eliminate data points lying outside the biomass supply area shown in Figure 3.

2. Land-cover categories that do not deliver any input for the process are excluded from the database.

3. Land-cover categories delivering the same sort of biomass are merged into one umbrella category

4. For each remaining category, we test whether there are any polygons larger than the desired maximum size. All polygons larger than the desired maximum size (here, 100km^2) are isolated.

5. The isolated polygons from each land-cover category are cut into smaller areas, using a so-called fishnet feature class consisting of 10x10 km squares; thus, the maximum possible size after this step is 100km^2.

6. The cut areas from step 5 are merged back with polygons that were originally < 100km^2.

7. The ArcGIS Feature to Point tool is used to calculate the centroid for each polygon in each land-cover category; the properties of the corresponding polygons, namely their area and type of land cover, are also stored.

8. The centroid's coordinates are determined and stored for each landcover category.

9. The information gathered for the points are exported into separate csv files for each land-cover category, containing each point's longitude ξ_j, latitude φ_j, type of land cover, and area.

10. All csv files are merged into one csv file containing all relevant biomass supply points and associated information.

11. The mass and energy of the biomass available at each biomass supply point is calculated using the specific yields given in Table 5.

The information in the resulting csv file is a crucial input for the algorithm: Each line in the file represents one $j \in J$ and has the following components: mass of biomass m_j, its energy content z_j, price pc_j and location $\{\xi_j,\varphi_j\}$.

Table 5: Availability of residual biomass per hectare

Biomass	Coverage	Yield (t/ha)	Energy content (MWh/t)	Purchasing cost pc_j (€/t)
Residual wood	Forest	1.0	4.3	70
Straw	Agriculture	5.0	4.0	35
Landscaping materials	Miscellaneous	1.5	5.5	40
Biowaste	City	3.5	0.9	360
Maintenance material	Parks and sport areas	6.0	1.4	200
Hay	Meadows	1.5	5.0	165
Leaves	Wine,fruit & olive trees	4.0	4.3	40

FNR, 2007; Fricke and Bahr, 2010; Hakala et al., 2009; IBS, 2015; Kaltschmitt, 2009; DBFZ, 2014; Zeller et al., 2012

In the course of these preparatory steps, the original 44 land cover categories are reduced to 21 that produce biomass, and these are condensed into seven categories defined by the seven kinds of residual biomass they yield (see Table 5). These land covers comprise the bulk of the dry land, an area of approximately 949,000km^2, represented by a total of 245,437 biomass supply points. Agricultural areas make up almost 45%, forests account for almost 33% of this area, meadows add 11% and urban areas another 6%. The remainder consists of scrub- and heathland, parks and sports facilities, as well as wine and fruit plantations.

1.4.2 Initializing the algorithm

As Figure 2 shows, before the ES/NLP loop can start, one must initialize the algorithm and generate starting solutions. First, the supply sources are imported from the csv file, which was prepared as previously described. Random valid solutions are then generated for the decision variables. ξ_{loc} and φ_{loc} are constructed using the CreateRandomPoints tool from ArcGIS, which creates random points inside any polygon, in this case, within the borders of Germany. The

starting capacity is randomly chosen between 1,000 MWh and 1,129 TWh of biomass input per year, which corresponds to an annual product output in tons of $31.25 \leq x_0 \leq 35{,}281{,}250$. Setting the lower bound to a value > 0 forces the algorithm to search for the least deficient biorefinery, in the case of a negative ROI, instead of simply setting $x_0 = 0$, resulting in an ROI of zero. The starting values of the strategy variables (σ) required for the ES are defined deterministically. For the location variables, they are set at $\sigma_{\xi loc} = \sigma_{\varphi loc} = 50{,}000$[m]. This indicates that the expected step length for the longitude and latitude variables is 50km when initializing the algorithm. The capacity strategy variable is set to σ_{x0}= 8,000,000 TWh of input biomass. The ES is self-adapting, lowering the expected step length in later stages to approach (local) optima accurately. μ = 15 starting solutions (individuals) of the form given in Equation 23 are created and subsequently passed on to the recombination step to generate λ = 100 children. Values of μ = 15 and λ = 100 are close to the recommended radio of μ/λ = 1/7 and are generally viewed as a well working standard setting in ES (Eiben and Smith,2015).

individual = (ξ_{loc}, φ_{loc}, x_0, $\sigma_{\xi loc}$, $\sigma_{\varphi loc}$, σ_{x0}).

1.4.3 Calculating the NLP and selecting the best solutions

The specific costs for biomass provision are given in Table 5. The transportation costs are set at *tv* = 0.25 €/tkm and *tf* = 3.69 €/t, averages from (Jenkins and Sutherland, 2014; Kerdoncuff, 2008). To estimate road distances traveled, the point cloud depicted in Figure 4 was derived by repeatedly comparing the Euclidean distance and the road distance as given by Google Maps. The potential regression through these points yields values of β = 1.6611 and γ = 0.959. These parameters account for the tendency that the discrepancy between Euclidean and road distance is larger for shorter distances, as Figure 4 shows.

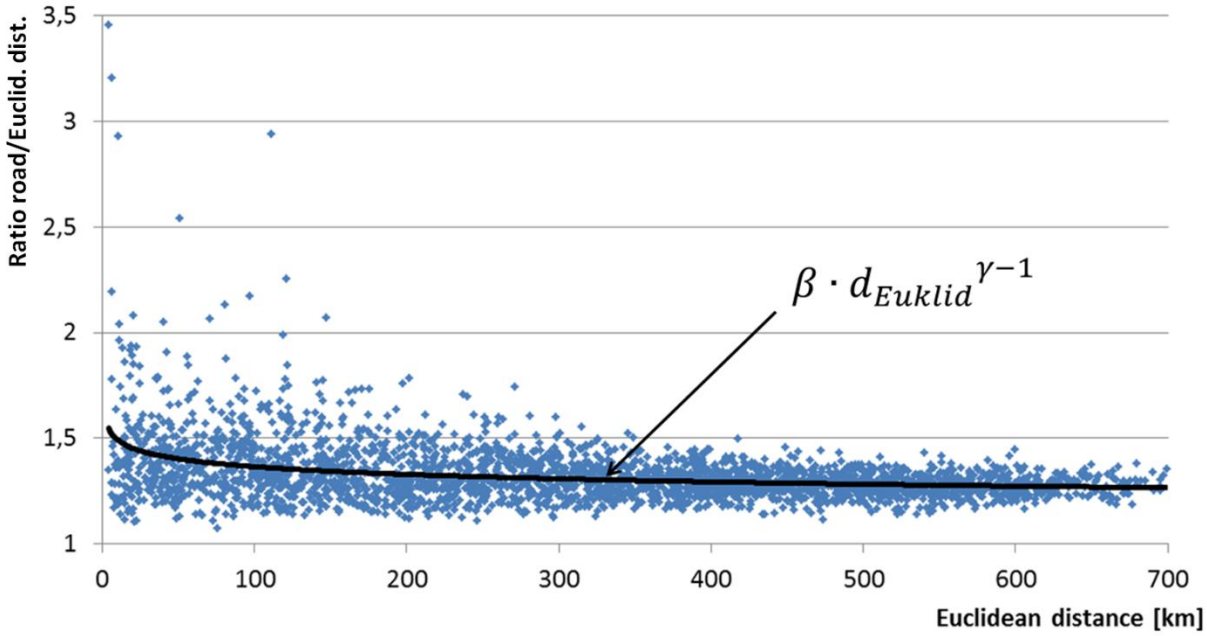

Figure 4: Relation Between Euclidean Distance and Distance on the Road

Given the fixed capacity x_0, the calculated biomass costs (*bc'*) associated with this capacity, and the location (ξ'_{loc}; φ'_{loc}), the NLP can now be solved. To account for plant cost escalation

from the time the investment data was published to the current level of prices in Germany, we use the Chemie Technik index with $\Psi = 1.3$. Furthermore, since each plant construction is also associated with numerous cost items linked indirectly to the construction (outside battery limits, OSBL; e.g., overhead, utilities), an OSBL-factor for these investments is set to $\Theta \approx 1.37$ (Peters et al., 2003). Because the plant is assumed to supply its own electricity, we also consider the percentage of synthesis products needed to cover this demand: $e = 5.11\%$ (Bechtel, 1998). As in similar natural gas-based plants, the capital charge rate is set to $f = 25\%$ (Derouane, 2005).

1.5 Results

To assess the algorithm's performance, we present our results for the synthesis gas biorefinery location, capacity, and configuration found with the aforementioned assumptions using GIS data for Germany. Figure 5 shows the convergence paths of the best objective function value of 50 algorithm applications. The algorithm's computation time is 3-3.5 hours on an Intel Core i5-3750 CPU with 3.4 GHz, 8 GB RAM, and Windows 7. It decreases to about 2.5 hours on an i7-4710 CPU with 3.4 GHz, 8 GB RAM, and Windows 8.1/10. Two tasks take up most of the calculation time. First, placing the biomass sources in ascending order according to their distances from the potential location is time-consuming. This task is performed using Python's sort-function for lists. Second, solving the NLP for the configuration variables in GAMS with the BARON solver. Although the half-second solution time does not seem long, it becomes a factor due to the number of calculations ($\lambda = 100$ for each of the 100 iterations).

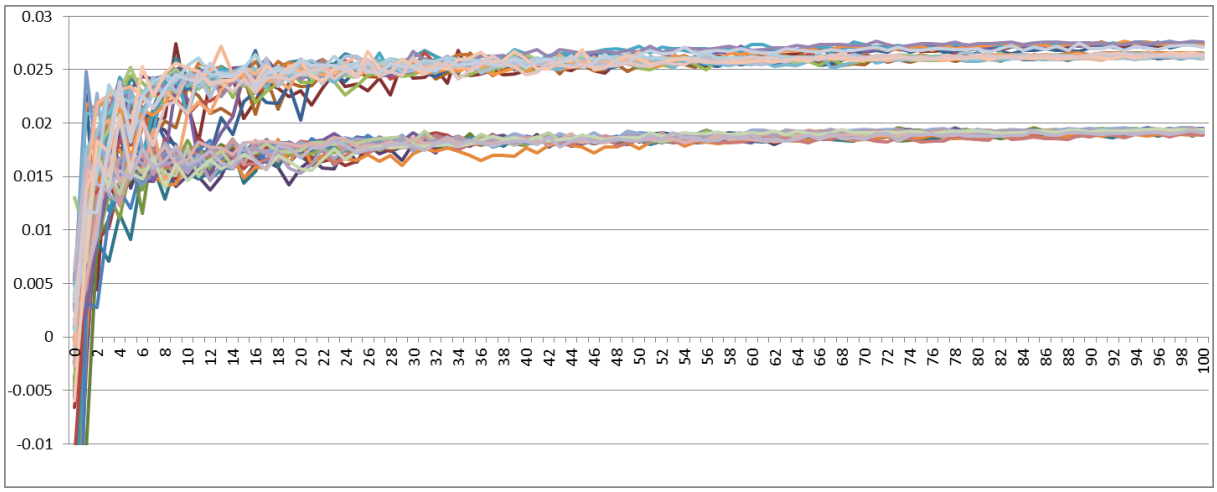

Figure 5: Development of the best objective function value in each generation in 50 runs.

1.5.1 Base scenario

In 50 runs, the algorithm converged toward three different solutions. All three show a positive objective function value, that is, an ROI greater than the requirement already included in the capital charge rate f (see Figure 5). The best solution (ROI = 2.75%) is located approximately 150 km east of Hamburg, in southern Mecklenburg-Western-Pomerania. Here, the capacity of 1,570,944 tons of final products per year corresponds to an annual biomass input of 50.3 million MWh. This solution is represented in Figure 6 by the center of the black northernmost circle, whose points indicate biomass sources. For this solution, 7,921 sources of residual

biomass from within a radius of 108 km supply the biorefinery with sufficient biomass. Two other solutions were also frequently returned as the best solution found in the 50 algorithm runs (see Table 6).

Table 6: ES-handled variable values for the best solutions found

Variable	Best solution	Second best	Third best
ROI	2.75%	2.63%	1.93%
ξ_{loc}	711,790.98	709,214.12	679,825.33
φ_{loc}	5,924,268.51	5,935,243.28	5,745,186.10
x_0	1,572,931.78	1,823,079.30	2,450,441.80

The second-best solution (ROI = 2.63%) has an identical configuration and is located only 10 km further north. It has a higher capacity of about 58.3 million MWh biomass input per year (x_0 = 1,823,079 tons). The third best solution, located near Halle/Saale in central Germany (see the southern location on the left in Figure 6) already shows a pronounced drop in ROI to 1.93%. Its capacity of 79 million MWh biomass input per year (x_0 = 2,450,448 tons) is about 50% larger than those of the other solutions.

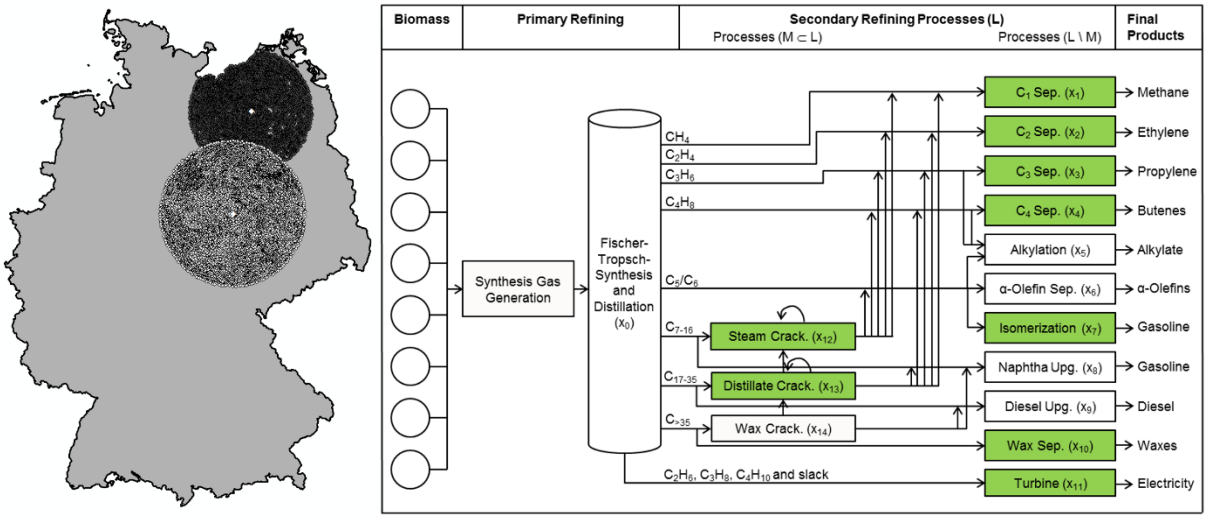

Figure 6: Best locations, required biomass sources (left) and selected upgrading units(right), all at maximum size for both locations.

This third solution apparently has a large convergence area, causing the algorithm to occasionally “get stuck" in this local optimum. In all three solutions, the relatively high chemical prices lead to a configuration focused on chemicals (see Table 7).

However, neither the expensive alkylation process (capacity x_5) nor fuel upgrading of naphtha or diesel hydrocarbons (capacities x_8 and x_9) is selected by the model. Instead, the model opts for the installation of the cracking processes to increase the production of chemicals such as ethylene, propylene and butenes. The only chemical separation not chosen is the α-olefin separation unit (capacity x_6), apparently because the high investment (see Table 13) cannot be justified by the expected increase in product value.

Table 7: Scenario and Sensitivity Analyses

Parameter	New value	ROI	ξ_{loc}	φ_{loc}	Input cap.	Config.
Base	-	2.8%	711 km	5924 km	50.3 TWh/a	chem.
tv	0.2 €/tkm	4.8%	821 km	5882 km	155.6 TWh/a	chem.
tv	0.2 €/tkm	0.1%	712 km	5924 km	50.3 TWh/a	chem.
f	20%	7.7%	711 km	5924 km	50.3 TWh/a	chem.
f	30%	-2.2%	711 km	5924 km	50.3 TWh/a	chem.
straw av.	3.75 t/ha	-1.1%	712 km	5924 km	39.8 TWh/a	chem.
straw av.	2.5 t/ha	-6.2%	716 km	5930 km	25.7 TWh/a	chem.
$sp_{2,3,4,6}$	$sp_{2,3,4,6} \cdot 0.95$	1.3%	712 km	5924 km	50.3 TWh/a	fuels
$\|J\|$	$\|J\| \cdot 1/3$	-15.6%	695 km	5921 km	19.7 TWh/a	chem.

As mentioned above, the algorithm does occasionally settle into evidently local optima (see Figure 5). This problem can be redressed by applying the algorithm several times to assess how reliably the algorithm obtains the same solution. This is, in fact, the standard procedure when applying heuristics (e.g. Kumar et al. (2014)). With the current ES parameters, the algorithm seems to deliver the second-best solution more frequently than the best solution. This outcome may be attributed to a larger catchment area for the second-best solution. As shown above, the area in which the best solution is better than the second best solution is very narrow.

To evaluate the quality of the solutions, we first develop a lower bound for the problem by fixing the configuration to one similar to that of Kreutz et al. (2008). The focus here is on fuels, as is often proposed in the literature (Kerdoncuff, 2008; Kreutz et al., 2008; Walther et al., 2012). With this fixed configuration, we optimize the location and capacity of the plant. Subsequently, we optimize the configuration for the location and capacity found. This procedure results in an ROI of -0.95%, well below the ROI of 2.75% of our integrated approach. This shows that for the investigated biorefinery, the simultaneous optimization of location, capacity, and configuration yields better results than a sequential optimization of the decision variables.

1.5.2 Sensitivity and scenario analysis

A sensitivity analysis of the best solution provides insights into the algorithm's ability to find narrow local optima. Toward this end, the location and capacity variables are independently altered from the best solution found. Subsequently, these new variable values are supplied to the NLP, which calculates the corresponding configuration and objective function value. All other things being equal, a change of 0.01% in the capacity domain reduces the objective function value to below that of the second-best solution. The objective function value is also sensitive to changes in the location variables. The algorithm must find an area of about 1 km^2 out of 357,376 km^2 within German borders, with a 0.02% range of the capacity domain in order to find a solution with a higher objective function value than the second-best solution. This illustrates the roughness of the objective function landscape. Finding the small convergence area for this solution several times thus appears to verify the soundness of the method.

To assess how sensitive the optimal solution is to a change in parameters, we analyzed eight altered scenarios (also see Figure 7 and Table 7 for results). Each scenario was calculated ten times to obtain sufficiently robust results. The availability of straw, the most significant biomass input in the original case study, was decreased to 75% and 50% of the original specific yield of 5 t per hectare. While the best locations found for both scenarios were only a few kilometers from the optimal location found originally, the achievable ROI decreased to -1.1% and -6.2%, respectively. The reduction of straw availability by 25% reduces the optimal capacity by 21.5%, while a 50% lower straw availability leads to a capacity reduction of 48.9%. The configuration remains the same, with a focus on chemicals production. In some of the algorithm runs with the lowest straw availability, another solution in southeastern Germany was also found, but with a distinctly lower ROI of -7.4%

The availability of residual biomass assumed in the original calculation was comparatively high, due to the assumption that all accruing biomass was available for the biorefinery. To reflect that demand from other biomass conversion plants may also compete for the same biomass, we randomly excluded two thirds of the biomass sources. This means that we randomly deleted two thirds of the 245,347 biomass supply points resulting from the input preparation steps described in Section 1.4.1. Thus, the number of biomass supply points in set J is reduced from said 245,347 to 81,782, also cutting the total available biomass roughly down to one third. The location found by the algorithm again remained stable, about 20 kilometers west of the original location, and had a comparable maximum transportation distance for the input biomass. The overall capacity x_0 of the plant was thus distinctly lower (about 20 TWh/yr of biomass input) and the plant ROI dropped to -15.6%. Repeated runs with new randomly selected 81,782 biomass supply points showed very similar results.

Figure 7: Graphic representation of selected scenario analyses

When we altered the variable transportation costs by 0.05 €/tkm to 0.3 €/tkm and 0.2 €/tkm, the configuration remained focused on chemicals and the location remained in the same region. The plant capacity, however, changed significantly (see Figure 7).

To investigate the effect of lower chemical prices, we reduced the selling prices sp_i for the bulk chemicals ethylene, propylene, butene and C_5/C_6-α-olefins by 5%. The result was a noticeable change in the configuration: The separation units for lower olefins (capacities x_2-x_4) were

significantly smaller, since no cracking units (capacities x_{12}-x_{14}) were installed. Instead, more fuel was upgraded (capacities x_8-x_9).

As Figure 7 and Table 9 show, the algorithm does indeed react to parameter changes as one would expect: the lower availability of straw does influence the capacity and profitability of the plant; lower variable transportation costs do lead to a much larger capacity with a larger supply area; and different product prices do lead to an adapted configuration. Nevertheless, for most of these scenarios, the location remains almost the same. Only large deviations in the capacity also seem to also alter the location of the plant.

1.6 Discussion

The results of this case study must be evaluated both from a theoretical and a practical point of view. While an algorithm with the ability to find narrow local optima for the objective function can be said to perform well from an OR point of view, the assessment of its results may differ from a practical business point of view. For example, a planner may choose a more robust solution with a slightly lower objective function value if the sensitivity of that solution is lower than that of the supposedly best solution. Because no real-life business case will ever be completely consistent with the assumptions made during the planning of a biorefinery, choosing a solution less sensitive to changes in parameter values may in fact be the better business decision.

Some of the locations identified by the algorithm, particularly the global optimum close to the Baltic Sea, the third best solution near Halle/Saale and the site closer to the Oder river are close to sites that either house existing bioenergy plants, such as the Bioenergiepark Güstrow, Germanys largest biomethane plant and a biorefinery at the Leuna chemical site, or have been considered for a BtL addition to the local mineral oil refinery in Schwedt/Oder. Under the assumption that straw is the primary input material, the findings of the algorithm therefore appear meaningful.

The reliability of the entire algorithm depends significantly on the reliability of the solver for the exact optimization of the biorefinery configuration. The BARON solver reliably solved the problem in all tests of our particular problem. The downside of the BARON solver is its relatively long run time. Other solvers, namely CONOPT, the Sparse Nonlinear OPTimizer (SNOPT), the Modular In-core Nonlinear Optimization System (MINOS), and the Nonlinear Interior point Trust Region Optimization (KNITRO), provide results more quickly, but do not always solve the problem to its global optimum. The approach could be improved once the performance of available nonlinear solvers makes it possible to reliably optimize more complex objective functions, such as net present value calculations, in manageable durations.

The presented combination of exact optimization algorithms, heuristics, and GIS shows that the development of information systems makes it possible to include an increasing number of aspects into the planning process and to address more complex problems using decision support models. The use and combination of extensive data stored in numerous established and novel databases is possible due to the steadily improving performance of computer hardware.

With even more potent hardware, it would also be possible to use actual road distances between the residual biomass collection points and the biorefinery. In this case, the approximation metric used in determining biomass related costs (*bc*) in Section 1.4.3 would have to be replaced with a shortest path algorithm performed on a street network spatial dataset. Although implementation with ArcGIS would be possible, the calculation time of the overall algorithm would severely increase (Brimberg et al., 2007; Hidaka and Okano, 2003). In the case study we introduced, the road distance would have to be calculated from each of the $\lambda = 100$ potential locations to (at least a significant share of) the 245,437 biomass sources we considered in each of the 100 generations. This amounts to about 2.5 billion shortest path calculations. Even if we only calculate the road distance to the 8,000 nearest biomass sources, 80 million shortest path calculations would be required.

1.7 Conclusion and outlook

We have presented an approach to integrate high-resolution data on the spatial availability of biomass inputs into the planning of a biorefinery using a combination of GIS, ES, and exact nonlinear optimization. For the case study investigated, the algorithm reliably converges and delivers good solutions to a problem that has not been previously considered in a comparable combination of extent, complexity, and resolution.

Although we validated our algorithm using a biorefinery application in Germany, it would be easy to adapt it to other geographical areas, given that appropriate land cover data is available. Because the CLC 2006 database we applied is available for all of Europe, application in European countries is clearly possible; data for other regions, such as Canada or the USA, is also available. However, the biomass yields and peculiarities of different available biomasses would have to be adapted. Another conceivable refinement may be to exclude certain areas from the biomass input dataset, e.g. when otherwise utilization of the considered biomass is established, or to add regionally differentiated biomass yields due to weather or soil conditions.

The algorithm's modular structure makes it possible to implement other biorefinery types by modeling their configuration in GAMS, while keeping the remainder of the algorithm in the ES essentially the same. Thus, depending on the biomass available in the investigated area, a compatible biorefinery for this biomass can be investigated easily, if a mathematical formulation of the biorefinery production processes is available.

An aspect which has been neglected so far is the uncertain availability of biomass supply (Wiedenmann and Geldermann, 2015; Borodin et al., 2016). However, the algorithm presented in this paper is suitable for the inclusion of stochastic availability, due to the large number of assessments of the objective function. Narrow solutions, such as the best solution found and presented in the Results section, are less likely to appear when stochastic biomass availability is incorporated into the algorithm.

Finally, the presented approach may also be applicable for other multiproduct production systems that are highly dependent on the spatial availability of inputs, such as agricultural food production or industrial wood processing plants.

Acknowledgements

This research was supported by the German Research Foundation (RTG), grant GRK 1703/1 for the Research Training Group “Resource Efficiency in Interorganizational Networks | Planning Methods to Utilize Renewable Resources". The authors wish to thank the three anonymous reviewers for their continuous efforts and numerous helpful comments which improved the paper significantly.

References

Ba, B. H., Prins, C., Prodhon, C., 2016. Models for optimization and performance evaluation of biomass supply chains: An operations research perspective. Renewable Energy 87, 977-989.

Bao, B., Ng, D. K., Tay, D. H., Jiménez-Gutiérrez, A., El-Halwagi, M. M., 2011. A shortcut method for the preliminary synthesis of process-technology pathways: An optimization approach and application for the conceptual design of integrated biorefineries. Computers & Chemical Engineering 35 (8), 1374-1383.

Bechtel, 1998. Aspen Process Flowsheet Simulation Model of a Battelle Biomass-Based Gasification, Fischer-Tropsch Liquefaction and Combined-Cycle Power Plant. Topical report for the US Department of Energy, Pittsburgh.

Berens, W., Körling, F.-J., 1985. Estimating road distances by mathematical functions. European Journal of Operational Research 21 (1), 54-56.

Borodin, V., Bourtembourg, J., Hnaien, F., Labadie, N., 2016. Handling uncertainty in agricultural supply chain management: A state of the art. European Journal of Operational Research 254 (2), 348-359.

Brimberg, J., Walker, J. H., Love, R. F., 2007. Estimation of travel distances with the weighted *l*p norm: Some empirical results. Journal of Transport Geography 15 (1), 62-72.

Chittenden, F., Derregia, M., 2015. Uncertainty, irreversibility and the use of `rules of thumb' in capital budgeting. The British Accounting Review 47 (3), 225-236.

Chu, W., Gao, X., Sorooshian, S., 2011. A new evolutionary search strategy for global optimization of high-dimensional problems. Information Sciences 181 (22), 4909-4927.

Comber, A., Dickie, J., Jarvis, C., Phillips, M., Tansey, K., 2015. Locating bioenergy facilities using a modified GIS-based location-allocation-algorithm: Considering the spatial distribution of resource supply. Applied Energy 154, 309-316.

Corsano, G., Vecchietti, A. R., Montagna, J. M., 2011. Optimal design for sustainable bioethanol supply chain considering detailed plant performance model. Computers & Chemical Engineering 35 (8), 1384-1398.

Derouane, E. G., 2005. Sustainable strategies for the upgrading of natural gas: Fundamentals, challenges, and opportunities. Vol. vol. 191 of NATO science series. Series II, Mathematics, physics, and chemistry. Springer, Dordrecht.

Dry, M. E., 2004. Chemical Concepts used for engineering purposes. In: Steynberg, A., Dry, M. (Eds.), Fischer-Tropsch Technology. Studies in Surface Science and Catalysis. Elesevier Science Publishers B.V, Amsterdam, 196-257.

Eiben, A. E., Smith, J. E., 2015. Introduction to evolutionary computing, second edition Edition. Natural Computing Series. Springer, Berlin Heidelberg.

Federal Government, 2012. Biorefineries Roadmap: as part of the German Federal Government action plans for the material and energetic utilization of renewable raw materials. URL http://www.bmel.de/SharedDocs/Downloads/Broschueren/ RoadmapBioraffinerien.pdf? _ blob=publicationFile . Accessed 20.01.17.

FNR, 2007. Leitfaden Bioenergie: Planung, Betrieb und Wirtschaftlichkeit von Bioenergieanlagen: [Bioenergy guidelines: Planning, operation and economics of bioenergy plants], 4th Edition. Fachagentur Nachwachsende Rohstoffe (FNR), Gülzow. URL http://www.worldcat.org/oclc/254367004

Fricke, K., Bahr, T., 2010. Sto_iche oder energetische Verwertung -die Wahl der Verwertungsart als Schlüssel zur Energieeffizienz: [Material or Energetic Usage - The Choice of Usage Options as the Key towards Energy Efficiency]. DWA-Bundestagung, Potsdam.

Geraili, A., Sharma, P., Romagnoli, J. A., 2014. A modeling framework for design of nonlinear renewable energy systems through integrated simulation modeling and metaheuristic optimization: Applications to biorefineries. Computers & Chemical Engineering 61, 102-117.

Gold, S., Seuring, S., 2011. Supply chain and logistics issues of bio-energy production. Journal of Cleaner Production 19 (1), 32-42.

Golembiewski, B., Sick, N., Bröring, S., 2015. The emerging research landscape on bioeconomy: What has been done so far and what is essential from a technology and innovation management perspective? Innovative Food Science & Emerging Technologies 29, 308-317.

Hakala, K., Kontturi, M., Pahkala, K., 2009. Field biomass as global energy source. Agricultural and Food Science 18, 347-365.

Hidaka, K., Okano, H., 2003. An approximation algorithm for a large-scale facility location problem. Algorithmica 35 (3), 216-224.

Horng, S.-C., Yang, F.-Y., Lin, S.-S., 2012. Embedding evolutionary strategy in ordinal optimization for hard optimization problems. Applied Mathematical Modelling 36 (8), 3753-3763.

IBS, 2015. Energetische Nutzung von Abfallprodukten: [Energetic Use of Waste Products]. URL http://energieberatung.ibs-hlk.de/plangetrei newsabfall.htm

Jenkins, T. L., Sutherland, J. W., 2014. A cost model for forest-based biofuel production and its application to optimal facility size determination. Forest Policy and Economics 38, 32-39.

Julstrom, B. A., 1999. Comparing darwinian, baldwinian, and Lamarckian search in a genetic algorithm for the 4-cycle problem. Late Breaking Papers at the 1999 Genetic and Evolutionary Computation Conference, 134-138.

Kaltschmitt, M. (Ed.), 2009. Energie aus Biomasse: Grundlagen, Techniken und Verfahren, 2nd Edition. Springer Verlag, Dordrecht and Heidelberg and London and New York and NY.

Kaundinya, D. P., Balachandra, P., Ravindranath, N. H., Ashok, V., 2013. A GIS (geographical information system)-based spatial data mining approach for optimal location and capacity planning of distributed biomass power generation facilities: A case study of Tumkur district, India. Energy 52, 77-88.

Kerdoncuff, P., 2008. Modellierung und Bewertung von Prozessketten zur Herstellung von Biokraftstoffen der zweiten Generation [Modelling and Assessment of Process Chains for the Production of Second Generation Biofuels]. Dissertation. Universitätsverlag Karlsruhe, Karlsruhe.

Kim, J., Real_, M. J., Lee, J. H., 2011a. Optimal design and global sensitivity analysis of biomass supply chain networks for biofuels under uncertainty. Computers & Chemical Engineering 35 (9), 1738-1751.

Kim, J., Real_, M. J., Lee, J. H., Whittaker, C., Furtner, L., 2011b. Design of biomass processing network for biofuel production using an MILP model. Biomass and Bioenergy 35 (2), 853-871.

Kreutz, T. G., Larson, E. D., Liu, G., Williams, R. H., 2008. Fischer-Tropsch Fuels from Coal and Biomass. 25th Annual International Pittsburgh Coal Conference, Pittsburgh and Pennsylvania and USA. URL http://web.mit.edu/mitei/docs/reports/kreutz-fischer-tropsch.pdf

Kumar, S., Kumar Sharma, V., Kumari, R., 2014. Memetic search in differential evolution algorithm. International Journal of Computer Applications 90 (6), 40-47.

Kurka, T., Jefferies, C., Blackwood, D., 2012. GIS-based location suitability of decentralized, medium scale bioenergy developments to estimate transport CO_2 emissions and costs. Biomass and Bioenergy 46, 366-379.

Langeveld, J., Sanders, J., 2010. General introduction: Prelude: why this book? In: Langeveld, H., Meeusen, M., Sanders, J. (Eds.), The bio-based economy. Earthscan, London and Washington, DC, 3-17.

Lauven, L.-P., 2014. An optimization approach to biorefinery setup planning. Biomass and Bioenergy 70, 440-451.

Leduc, S., Schwab, D., Dotzauer, E., Schmid, E., Obersteiner, M., 2008. Optimal location of wood gasi_cation plants for methanol production with heat recovery. International Journal of Energy Research 32 (12), 1080-1091.

Leduc, S., Starfelt, F., Dotzauer, E., Kindermann, G., McCallum, I., Obersteiner, M., Lundgren, J., 2010. Optimal location of lignocellulosic ethanol refineries with polygeneration in Sweden. Energy 35 (6), 2709-2716.

Lin, T., Rodríguez, L. F., Shastri, Y. N., Hansen, A. C., Ting, K. C., 2013. GIS-enabled biomass-ethanol supply chain optimization: model development and Miscanthus application. Biofuels, Bioproducts and Biorefining 7 (3), 314-333.

Lin, T., Wang, S., Rodríguez, L. F., Hu, H., Liu, Y., 2015. Gis-enabled decision support platform for biomass supply chain optimization. Environmental Modelling & Software 70, 138-148.

Mahdavi, S., Shiri, M. E., Rahnamayan, S., 2015. Metaheuristics in largescale global continues optimization: A survey. Information Sciences 295, 407-428.

Mansoornejad, B., Chambost, V., Stuart, P., 2010. Integrating product portfolio design and supply chain design for the forest biorefinery. Computers & Chemical Engineering 34 (9), 1497-1506.

Melo, M. T., Nickel, S., Saldanha-da Gama, F., 2009. Facility location and supply chain management - A review. European Journal of Operational Research 196 (2), 401-412.

Michalewicz, Z., Fogel, D. B., 2000. How to solve it: Modern heuristics.Springer, Berlin and New York.

Muñoz, M. A., Sun, Y., Kirley, M., Halgamuge, S. K., 2015. Algorithm selection for black-box continuous optimization problems: A survey on methods and challenges. Information Sciences 317, 224-245.

Natarajan, K., Leduc, S., Pelkonen, P., Tomppo, E., Dotzauer, E., 2014. Optimal locations for second generation Fischer Tropsch biodiesel production in Finland. Renewable Energy 62, 319-330.

Ochsner, H., 2010. Bioenergie aus der Landschaftspege: [Bioenergy from Landscape Preservation].

Omidvar, M. N., Li, X., Tang, K., 2015. Designing benchmark problems for large-scale continuous optimization. Information Sciences 316, 419-436.

Owen, S. H., Daskin, M. S., 1998. Strategic facility location: A review. European Journal of Operational Research 111 (3), 423-447.

Peters, M. S., Timmerhaus, K. D., West, R. E., 2003. Plant design and economics for chemical engineers, 6th Edition. McGraw-Hill Inc, New York.URL http://www.worldcat.org/oclc/50410278

Pohlheim, H., 1999. Evolutionäre Algorithmen: Verfahren, Operatoren und Hinweise für die Praxis: [Evolutionary Algorithms: Methods, operators and advice for practical applications]. VDI-Buch. Springer Verlag, Berlin.

Reche-López, P., Ruiz-Reyes, N., Garca Galn, S., Jurado, F., 2009. Comparison of metaheuristic techniques to determine optimal placement of biomass power plants. Energy Conversion and Management 50 (8), 2020-2028.

Rechenberg, I., 1973. Evolutionsstrategie; Optimierung technischer Systeme nach Prinzipien der biologischen Evolution: [Evolutionary strategy: Optimization of technical systems according to the principles of biological evolution]. Vol. 15 of Problemata. Frommann-Holzboog, Stuttgart.

Rechenberg, I., 1994. Evolutionsstrategie '94: [Evolutionary strategy '94]. Vol. Bd. 1 of Werkstatt Bionik und Evolutionstechnik. Frommann-Holzboog, Stuttgart.

Regis, R. G., 2010. Convergence guarantees for generalized adaptive stochastic search methods for continuous global optimization. European Journal of Operational Research 207 (3), 1187-1202.

Rentizelas, A. A., Tatsiopoulos, I. P., 2010. Locating a bioenergy facility using a hybrid optimization method. International Journal of Production Economics 123 (1), 196-209.

ReVelle, C. S., Eiselt, H. A., 2005. Location analysis: A synthesis and survey. European Journal of Operational Research 165 (1), 1-19.

Sahinidis, N. V., 2014. BARON 14.3.1: Global Optimization of Mixed-Integer Nonlinear Programs, User's Manual.

Santibañez-Aguilar, J. E., González-Campos, J. B., Ponce-Ortega, J. M.,Serna-González, M., El-Halwagi, M. M., 2014. Optimal planning and site selection for distributed multiproduct biorefineries involving economic, environmental and social objectives. Journal of Cleaner Production 65, 270-294.

Sayed, E., Essam, D., Sarker, R., Elsayed, S., 2015. Decomposition-based evolutionary algorithm for large scale constrained problems. Information Sciences 316, 457-486.

Schaidle, J. A., Moline, C. J., Savage, P. E., 2011. Biorefinery sustainability assessment. Environmental Progress & Sustainable Energy 30 (4), 743-753.

Sen, S. M., Binder, J. B., Raines, R. T., Maravelias, C. T., 2012. Conversion of biomass to sugars via ionic liquid hydrolysis: process synthesis and economic evaluation. Biofuels, Bioproducts and Biorefining 6 (4), 444-452.

Sharma, P., Vlosky, R., Romagnoli, J. A., 2013. Strategic value optimization and analysis of multi-product biomass refineries with multiple stakeholder considerations. Computers & Chemical Engineering 50, 105-129.

Staffas, L., Gustavsson, M., McCormick, K., 2013. Strategies and policies for the bioeconomy and bio-based economy: An analysis of official national approaches. Sustainability 5 (6), 2751-2769.

Tawarmalani, M., Sahinidis, N. V., 2005. A polyhedral branch-and-cut approach to global optimization. Mathematical Programming 103, 225-249.

Thomas, A., Bond, A., Hiscock, K., 2013. A GIS based assessment of bioenergy potential in England within existing energy systems. Biomass and Bioenergy 55, 107-121.

Thomsen, R., 2003. Flexible ligand docking using evolutionary algorithms: investigating the effects of variation operators and local search hybrids. Biosystems 72 (1-2), 57-73.

Tijmensen, M., Faaij, A., Hamelinck, C. N., van Hardeveld, M., 2002. Exploration of the possibilities for production of _scher tropsch liquids and power via biomass gasi_cation. Biomass and Bioenergy 23 (2), 129-152.

Towler, G. P., Sinnott, R. K., 2013. Chemical engineering design: Principles, practice and economics of plant and process design, second edition, 2nd Edition. Butterworth Heinemann, Kidlington and Oxford and U.K and Waltham and Mass.

Umweltbundesamt, 2009. CORINE Land Cover (CLC2006). Umweltbundesamt.

Vera, D., Carabias, J., Jurado, F., Ruiz-Reyes, N., 2010. A Honey Bee Foraging approach for optimal location of a biomass power plant. Applied Energy 87 (7), 2119-2127.

Vesterstrom, J., Thomsen, R., 2004. A comparative study of differential evolution, particle swarm optimization, and evolutionary algorithms on numerical benchmark problems. In: IEEE (Ed.), 2004 Congress on Evolutionary Computation. pp. 1980-1987.

Walther, G., Schatka, A., Spengler, T. S., 2012. Design of regional production networks for second generation synthetic bio-fuel: A case study in Northern Germany. European Journal of Operational Research 218 (1), 280-292.

Wang, L., Agyemang, S. A., Amini, H., Shahbazi, A., 2015. Mathematical modeling of production and biorefinery of energy crops. Renewable and Sustainable Energy Reviews 43, 530-544.

Wiedenmann, S., Geldermann, J., 2015. Supply Planning for Processors of Agricultural Raw Materials. European Journal of Operational Research 242 (2), 606-619.

Zeller, V., Thrän, D., Zeymer, M., Bürzle, B., Adler, P., Ponitka, J., Postel, J., Müller-Langer, F., Rönsch, S., Gröngröft, A., Kirsten, C., Weller, N., Schenker, M., Wedwitschka, H., Wagner, B., Deumeland, P., Reinicke, F., Vetter, A., Weiser, C., Henneberg, K., Wiegmann, K., 2012. DBFZ Report Nr. 13: Basisinformationen für eine nachhaltige Nutzung von landwirtschaftlichen Reststoffen zur Bioenergiebereitstellung. Leipzig.

Zhang, F., Johnson, D. M., Sutherland, J. W., 2011. A GIS-based method for identifying the optimal location for a facility to convert forest biomass to biofuel. Biomass and Bioenergy 35, 3951-3961.